NEOPLASIA
www.neoplasia.com

Volume 14 Number 7 July 2012 pp. 612–623 612

The Effect of Bevacizumab on Human Malignant Melanoma Cells with Functional VEGF/VEGFR2 Autocrine and Intracrine Signaling Loops[1,2]

Una Adamcic, Karolina Skowronski, Craig Peters, Jodi Morrison and Brenda L. Coomber

Department of Biomedical Sciences, Ontario Veterinary College, University of Guelph, Guelph, Ontario, Canada

Abstract

Receptors for the angiogenic factor VEGF are expressed by tumor cancer cells including melanoma, although their functionality remains unclear. Paired human melanoma cell lines WM115 and WM239 were used to investigate differences in expression and functionality of VEGF and VEGFR2 *in vitro* and *in vivo* with the anti-VEGF antibody bevacizumab. Both WM115 and WM239 cells expressed VEGF and VEGFR2, the levels of which were modulated by hypoxia. Detection of native and phosphorylated VEGFR2 in subcellular fractions under serum-free conditions showed the presence of a functional autocrine as well as intracrine VEGF/VEGFR2 signaling loops. Interestingly, treatment of WM115 and WM239 cells with increasing doses of bevacizumab (0-300 μg/ml) *in vitro* did not show any significant inhibition of VEGFR2 phosphorylation. Small-molecule tyrosine kinase inhibitor, sunitinib, caused an inhibition of VEGFR2 phosphorylation in WM239 but not in WM115 cells. An increase in cell proliferation was observed in WM115 cells treated with bevacizumab, whereas sunitinib inhibited proliferation. When xenografted to immune-deficient mice, we found bevacizumab to be an effective antiangiogenic but not antitumorigenic agent for both cell lines. Because bevacizumab is unable to neutralize murine VEGF, this supports a paracrine angiogenic response. We propose that the failure of bevacizumab to generate an antitumorigenic effect may be related to its generation of enhanced autocrine/intracrine signaling in the cancer cells themselves. Collectively, these results suggest that, for cancers with intracrine VEGF/VEGFR2 signaling loops, small-molecule inhibitors of VEGFR2 may be more effective than neutralizing antibodies at disease control.

Neoplasia (2012) 14, 612–623

Introduction

Vascular endothelial growth factor (VEGF-A) is an important regulator of both normal and pathologic angiogenesis [1,2]. To date, bevacizumab (Avastin), an anti-VEGF antibody, alone or in combination with chemotherapy, has shown clinical activity in colorectal [3,4], breast [5,6], ovarian [7], non–small cell lung [8], metastatic renal cell carcinoma [9], and glioblastoma multiforme [10], validating VEGF pathway inhibitors as an important treatment modality in cancer therapy [11]. Phase 2 studies of metastatic malignant melanoma report that up to 25% of patients with advanced cancer may show prolonged disease stabilization [12], and most studies demonstrate that bevacizumab in combination with chemotherapy or immune therapy shows moderate activity [13,14]. Sunitinib or SU11248 (Sutent; Pfizer) is an oral multitargeted tyrosine kinase inhibitor that inhibits phosphorylation of a variety of tyrosine kinases such as VEGFR1-3, and platelet-derived growth factor receptor β [15]. Sunitinib is effective as an antiangiogenic and antitumor reagent in both preclinical mouse models [16] and human clinical trials

Address all correspondence to: Brenda L. Coomber, PhD, Department of Biomedical Sciences, Ontario Veterinary College, University of Guelph, 50 Stone Rd E, Guelph, Ontario, Canada N1G 2W1. E-mail: bcoomber@uoguelph.ca

[1]This study was funded by grants from the Canadian Institutes for Health Research (MOP-81213) and a Canadian Cancer Society Research Institute (no. 20094). The authors declare no conflict of interest.

[2]This article refers to supplementary material, which is designated by Table W1 and is available online at www.neoplasia.com.

Received 8 July 2011; Revised 21 June 2012; Accepted 25 June 2012

DOI 10.1593/neo.11948

of non–small lung cancer [17], breast cancer [18], metastatic renal cancer [19], and other tumor types.

Within solid tumors, VEGF is mainly produced by cancer cells, and it binds in paracrine fashion to endothelial VEGFR1 (Flt-1), VEGFR2 (KDR, human/Flk-1, mouse), and neuropilin receptors (NRP1 and NRP2) [20]. VEGFR2 is responsible for most downstream angiogenic effects of VEGF including changes in vascular permeability, endothelial proliferation, invasion, migration, and survival [21]. Binding of VEGF to VEGFR2 also activates downstream survival and migration pathways involving PI3-kinase/Akt and focal adhesion kinase, respectively [22].

In addition to these paracrine functions, VEGF may also be involved in autocrine stimulation of tumor growth, binding specifically to VEGFRs present on cancer cells themselves [23–26]. The presence of VEGF receptors on human melanoma cells suggests the possibility of an autocrine VEGF/VEGFR signaling loop in this disease [27–29]. Overexpression of $VEGF_{165}$ in a melanoma cell line that expresses VEGFR2 favors cell growth and survival through MAPK and PI3K signaling pathways [27]. Some VEGF receptors may not be expressed on the surface of the cancer cells but instead remain intracellular, promoting survival through a VEGF/VEGFR "intracrine" mechanism [27,30,31].

Here we used the paired human melanoma cell lines (WM115 and WM239) [32] to investigate differences in expression of VEGF and VEGFR2. We identified autocrine as well as intracrine VEGF/VEGFR2 signaling in both primary (WM115) and metastatic (WM239) melanoma cell lines and investigated the signaling of these pathways and their possible impact on tumor responses to VEGF targeted therapy using xenografted cells.

Materials and Methods

Cell Lines and Culture Conditions

The following cell lines were purchased from American Type Culture Collection (Manassas, VA) and used in experiments — WM115 (primary melanoma [32]), WM239 (metastatic melanoma, isolated from a secondary lesion from the same patient [32]), bEnd3 (a mouse brain-derived polyoma middle T antigen-transformed endothelial cell line), and 293T (human fetal kidney) [33]. Primary bovine aortic endothelial cells (BAECs) were isolated from aorta of adult cattle and characterized as previously reported [34]. Human umbilical vein endothelial cells (HUVECs) were purchased from Lonza (Allendale, NJ). Cells were routinely cultured in Dulbecco modified Eagle medium (DMEM; Sigma-Aldrich, Mississauga, Canada) supplemented with 10% fetal bovine serum (FBS; Life Technologies, Burlington, Canada), sodium pyruvate (Sigma-Aldrich), and gentamicin (Life Technologies) at 37°C in 5% CO_2 and 95% air.

Reverse Transcription–Polymerase Chain Reaction

Confluent cultures of WM115 and WM239, 293T, and bENd3 cells were lysed using TriPure (Roche, Mississauga, Canada) and 5 μg of total RNA was used for complementary DNA (cDNA) synthesis with the Turbo DNAse kit (Amgen, Streetsville, Canada). Reverse transcription–polymerase chain reaction was performed for 30 cycles of 95°C for 1 minute, 60°C for 1 minute, and 72°C for 2 minutes. The polymerase chain reaction products were separated using 2% agarose gel electrophoresis. Primer sequences for human and mouse VEGFR2 were 5′-CCAAGAACTCCATGCCCTTA-3′ for the antisense and 5′-ATCCCTGTGGATCTGAAACG-3′ for the sense strand. Negative controls were performed on samples containing no reverse transcriptase enzyme and using reaction buffer without cDNA template.

Establishment of Tumor Xenografts

All procedures described below were done according to the guidelines and recommendations of the Canadian Council of Animal Care and approved by the University of Guelph Local Animal Care Committee. Tumor xenografts were established in 8-week-old female athymic nude mice (Charles River, Sherbrooke, Canada) by injecting 2×10^6 of WM115 or WM239 melanoma cells in 100 μl of 0.1% bovine serum albumin (BSA) subcutaneously into the right flank. Tumor growth was measured twice weekly using calipers, and tumor size was calculated using the equation: volume = length × width^2 × 0.5. Once tumors reached approximately 100 mm^3 in size, mice were randomly allocated into control or treatment group, eight per group. Groups were treated for 14 (WM115 xenografts) or 21 (WM239 xenografts) days with bevacizumab as Avastin intraperitoneally, 5 mg/kg twice weekly; mice in control groups received 100 μl of phosphate-buffered saline (PBS) twice weekly. Mice were killed by CO_2 asphyxiation followed by cervical dislocation. Tumors were removed from the surrounding tissue, embedded in OCT cryomatrix and snap frozen in liquid nitrogen or snap frozen in liquid nitrogen for future protein and RNA isolation, and stored at −80°C.

Western Blot Analysis

Cultured cell lines (WM115, WM239, and BAECs) were seeded at the appropriate densities and allowed to attach overnight in DMEM (Sigma-Aldrich) plus 10% FBS (Life Technologies). To be certain that phosphorylation of VEGFR2 is achieved through production of VEGF ligand by melanoma cells themselves and not by VEGF supplied in added serum, cells were thoroughly washed in PBS and serum-starved for 48 hours. Melanoma cells were treated with control human IgG antibody or 150 μg/ml of bevacizumab (Avastin) for 15 or 30 minutes before lysis. Cells were also incubated in a modular hypoxic chamber (Billups-Rothenberg, Del Mar, CA) under less than 0.01% oxygen for 24 and 48 hours and then lysed in protein lysis buffer containing Na_3VO_4 and phosphatase inhibitor cocktail 2, according to the manufacturer's instructions (Sigma-Aldrich). Cells were treated with 1 mM pervanadate for 30 minutes before lysis, and nuclear and cytosolic fractions were collected using the Nuclear and Cytosolic Fractionation kit (LabVision, Kalamazoo, MI). Frozen tumor pieces from WM115 and WM239 xenografts were disrupted in freshly prepared lysis buffer (Cell Signaling, Danvers, MA), and total protein lysates were electrophoretically resolved on 7.5% polyacrylamide gels and transferred to a polyvinylidene fluoride membrane (Roche). Membranes were blocked in 5% milk or 5% BSA (Jackson ImmunoResearch, West Grove, PA) in TBS/Triton followed by overnight incubation at 4°C in primary antibodies diluted in 5% milk or 5% BSA in TBS/Triton. Primary antibodies used were rabbit anti-VEGFR2, rabbit anti–phospho-VEGFR2 Tyr951, rabbit anti–phospho-VEGFR2 Tyr1175 (all 1:1000 dilution; all Cell Signaling Technology), mouse anti–α-tubulin (1:400,000; Sigma-Aldrich), and rabbit anti-lamin (1:1000; Cell Signaling Technology). Membranes were washed and treated with appropriate POD-conjugated secondary antibody (anti-rabbit POD at 1:10,000 and anti-mouse POD at 1:40,000; Sigma-Aldrich) and immunocomplexes visualized using a chemiluminescence

detection kit (Roche), exposed to an x-ray film and quantified on a FluorChem 9900 gel documentation imaging system (Alpha Innotech, San Leandro, CA). Protein loading was normalized using α-tubulin bands from protein lysates.

Nuclear/Cytosolic Fractions

Cultured cell lines (WM115, WM239, and BAECs) were seeded at the appropriate densities, allowed to attach overnight in DMEM (Sigma-Aldrich) plus 10% FBS (Life Technologies), and then thoroughly washed in PBS and serum-starved for 48 hours. Cells were rinsed once with PBS and fresh serum-free medium containing 1 mM pervanadate was added to cells 30 minutes before lysis. Melanoma cells were treated with 0 or 50 μg/ml bevacizumab as Avastin, with and without 5 ng/ml human recombinant VEGF (Life Technologies) for 15 or 30 minutes. Nuclear and cytosolic fractions were collected using the Nuclear and Cytosolic Fractionation kit (LabVision).

Dose Response

Cultured cell lines (WM115, WM239, and BAECs) were seeded at the appropriate densities, allowed to attach overnight in DMEM (Sigma-Aldrich) plus 10% FBS (Life Technologies), and then thoroughly washed in PBS and serum-starved for 48 hours. Cells were rinsed once with PBS and fresh serum-free medium containing 1 mM pervanadate was added to cells 30 minutes before lysis. Melanoma cells were treated with 0, 50, 150, and 300 μg/ml bevacizumab as Avastin or 0, 10, 100, or 300 nM sunitinib (Sigma-Aldrich), with and without 10 and 5 ng/ml human recombinant VEGF (Life Technologies), respectively, for 15 minutes. Cells were lysed in protein lysis buffer containing Na_3VO_4 and phosphatase inhibitor cocktail 2, according to the manufacturer's instructions (Sigma-Aldrich). Protein lysates were electrophoretically resolved on 7.5% polyacrylamide gels and transferred to a polyvinylidene fluoride membrane (Roche). Membranes were blocked in 5% milk or 5% BSA (Santa Cruz Biotechnologies, Santa Cruz, CA) followed by overnight incubation at 40°C in primary antibodies diluted in 5% milk or 5% BSA in TBS/Triton. Primary antibodies used were rabbit anti-VEGFR2, rabbit anti–phospho-VEGFR2 Tyr951, rabbit anti–phospho-VEGFR2 Tyr1175, (all 1:2000 dilution; all Cell Signaling Technology), mouse anti–α-tubulin (1:400,000; Sigma-Aldrich), and rabbit anti-lamin (1:1000, Cell Signaling Technology). Membranes were washed and treated with appropriate POD-conjugated secondary antibody (anti-rabbit POD at 1:20,000 and anti-mouse POD at 1:20,000; Sigma-Aldrich), and immunocomplexes were visualized using Luminata Western HRP Chemiluminescence Substrate (Millipore), exposed to an x-ray film, and quantified on a FluorChem 9900 gel documentation imaging system (Alpha Immunotech). Protein loading was normalized using α-tubulin bands from protein lysates.

Crystal Violet Assay

Cultured cell lines (WM115 and WM239) were seeded at the appropriate densities and allowed to attach overnight in DMEM (Sigma-Aldrich) plus 10% FBS (Life Technologies). Cells were treated with 0, 10, 100, or 300 nM sunitinib or 0, 50, 150, or 300 μg/ml bevacizumab in DMEM plus 1% FBS for 6 days, replacing the medium every 2 to 3 days. Cells were fixed and stained in 1% Crystal Violet, 20% methanol for 20 minutes at room temperature and rinsed multiple times with distilled H_2O. Once completely dried, stained cells were dissolved in 10% acetic acid for 20 to 30 minutes at room temperature and absorbance at 570 nm was determined.

Measurement of Human VEGF Protein Levels

A human VEGF ELISA kit (R&D Systems, Inc, Minneapolis, MN) was used to quantify VEGF in serum-free conditioned medium from WM115 and WM239 cells. Serum-starved cells were treated with control human IgG antibody, 50 or 150 μg/ml of bevacizumab as Avastin. Conditioned medium was collected 6 and 24 hours later and used immediately or stored at 4°C until VEGF quantification. Measurement of VEGF protein levels was performed on ELX800 (BioTek, Winooski, VT) plate reader. Adherent cells were trypsinized and counted using a hemocytometer for normalization purposes. VEGF ELISA was also used to quantify levels in lysed tumor xenografts from each of the treatment groups (control and bevacizumab) and normalized to total protein.

Immunofluorescence for Phosphorylated and Native VEGFR2 Receptor in Cultured Cells

WM115 and WM239 cells were cultured on sterile glass coverslips for 48 hours and exposed to 10 ng/ml VEGF or vehicle for 1 hour time. Coverslips were then fixed with 4% paraformaldehyde (USB Corporation, Cleveland, OH) at room temperature and permeabilized in 0.3% Triton X-100, and nonspecific binding was blocked using protein block (Dako, Burlington, Canada) for 30 minutes. Cells were incubated in rabbit anti-VEGFR2 antibody (Cell Signaling Technology) diluted 1:50 in PBS with 0.3% Triton X-100 overnight at 4°C or rabbit phospho-VEGFR2 Tyr951 (Cell Signaling Technology) at 1:400, followed by fluorescently tagged anti-rabbit Cy3 secondary antibody (1:200; Jackson ImmunoResearch) for 30 minutes. Slides were counterstained with DAPI (Dako) and mounted using fluorescent mounting medium (Dako). Images were captured with a 20× objective using QCapture software calibrated to a Leica DMLB microscope (Leica, Wetzlar, Germany) fitted with a QImaging QICAM fast1394 digital camera (QImaging, Surrey, Canada). Images were merged using Adobe Photoshop 7.0 (Adobe).

Blood Vessel Density Quantification

To determine blood vessel density, two blocks from each tumor xenograft were assessed. Cryosections, 8 μm thick, were fixed in 50:50 acetone-methanol mix for 10 minutes at −20°C and air-dried. Sections were rehydrated in PBS, and nonspecific binding was blocked using Dako protein-free block (Dako) for 1 hour followed by 1 hour in rat anti-CD31 antibody (1:50; Hyclone, Logan, UT) and then 30 minutes in donkey anti-rat FITC (1:200; Jackson ImmunoResearch). Slides were counterstained with DAPI and mounted as described. Sections were examined by epifluorescence microscopy, and images were captured with a 20× objective in a blinded fashion. Optimas 6.2 image analysis software program (MediaCybernetics, San Diego, CA) was used to determine the total number of blood vessels for each field to obtain the blood vessel density.

Statistical Analysis

Calculation of preliminary summary statistics such as mean, SD, and SE as well as graphing all the data was completed using Microsoft Excel (Microsoft Corp, Mississauga, Canada). On all samples, Grubbs' test, also called the ESD method (extreme studentized deviate), was used to determine significant outliers. Once outliers, if any, were identified and omitted from the analysis, analysis of variance was perform to determine the significance within and between groups ($P < .05$). Least

significant difference (Tukey) test was used to determine whether there were significant differences between groups. Data were presented as mean, SE, and range.

Results

VEGF and VEGFR2 Expression in Melanoma Cell Lines

Using ELISA, we detected the expression of VEGF in both WM115 and WM239 melanoma cell lines and observed an approximately 10-fold increase in the production of VEGF by metastatic (WM239) compared with primary (WM115) melanoma cells (Figure 1, *A* and *B*). The humanized anti-VEGF antibody bevacizumab was able to significantly neutralize available VEGF in the conditioned medium of WM115 cells by 24 hours (at 150 μg/ml, $P < .05$; Figure 1*A*) and of WM239 cells after 6 and 24 hours (at 50 and 150 μg/ml, $P < .05$; Figure 1*B*). VEGFR2 mRNA was detected in both primary and metastatic melanoma cell lines (Figure 1*C*). Western blot analysis confirmed the expression of VEGFR2 protein in both cell lines; WM115 cells express approximately 40% to 50% less VEGFR2 protein than BAECs, whereas WM239 melanoma cells express approximately 80% to 90% less VEGFR2 protein than BAECs ($P < .05$; Figure 1*D*). Also, there was significantly higher VEGFR2 expression in WM115 primary than in WM239 metastatic melanoma cells ($P < .05$; Figure 1*D*).

Functional Autocrine and Intracrine VEGF/VEGFR2 Signaling Loops

Once the presence and the relative amounts of the VEGF ligand and its receptor VEGFR2 were determined, we investigated the existence

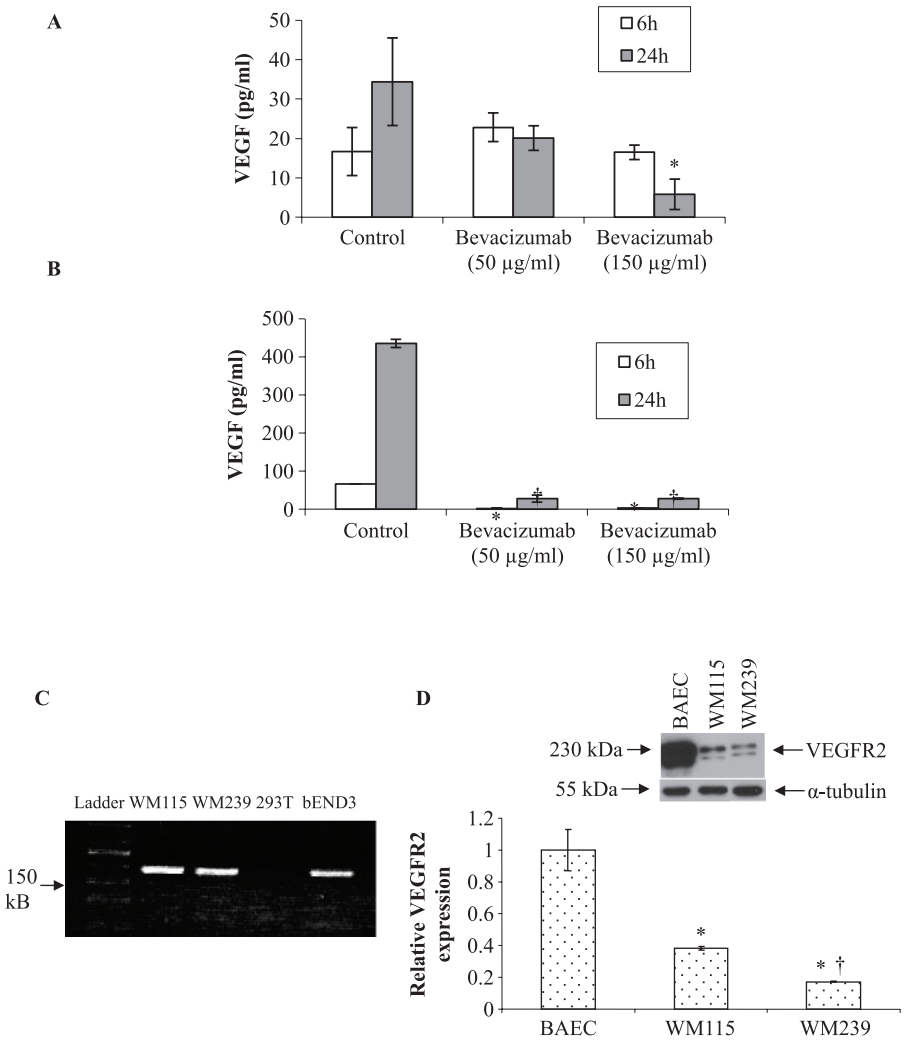

Figure 1. Expression of VEGF and VEGFR2 in melanoma cell lines *in vitro*. (A) Levels of VEGF ligand were measured in serum-free CM of primary (WM115) and (B) metastatic melanoma cell line (WM239) which were treated with bevacizumab (50 and 150 μg/ml) or control IgG. Graphs show that metastatic melanoma cells (WM239) have significantly upregulated VEGF expression compared with primary melanoma cells (WM115). In addition, significant inhibition of VEGF was observed in WM115 and WM239 cell lines treated with bevacizumab (50 or 150 μg/ml) compared with controls (50 μg/ml: $^*P < .05$; 150 μg/ml: $^\dagger P < .05$). $n = 3$. (C) Agarose gel stained with ethidium bromide showing VEGFR2 cDNA amplicons in both primary (WM115) and metastatic (WM239) melanoma cell lines. Human fetal kidney (293T) and mouse brain microvascular cells (bENd3) were used as negative and positive control, respectively. (D) A representative Western blot of VEGFR2 protein expressed by BAECs (positive control), WM115, and WM239 cells. α-Tubulin was used for normalization purposes. Densitometry of these blots shows significant differences in the expression of VEGFR2 in melanoma cell lines compared to each other ($^\dagger P < .05$) as well as control ($^*P < .05$). $n = 3$.

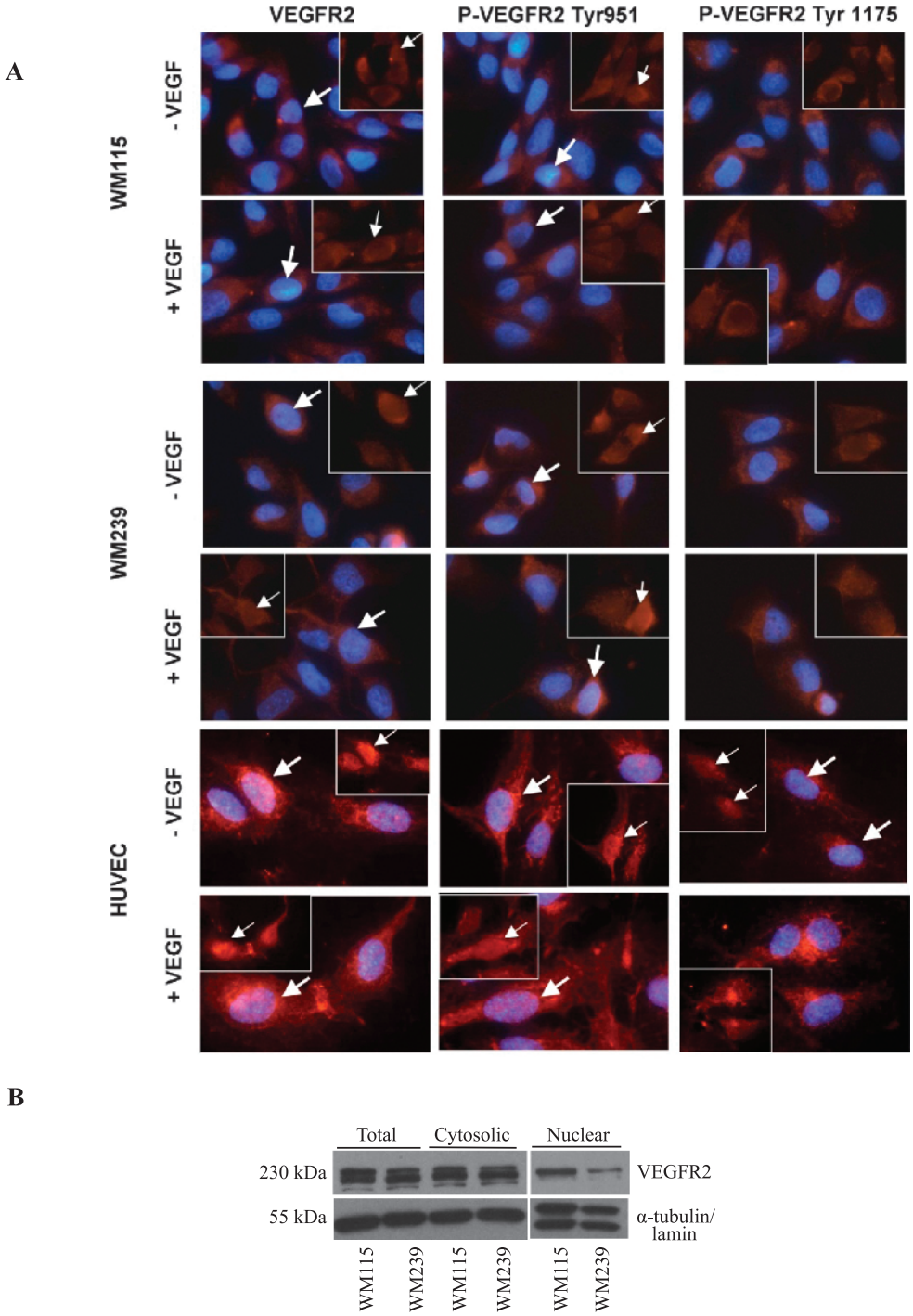

Figure 2. Detection of phosphorylated VEGFR2 and native VEGFR2 receptor. (A) Immunofluorescent staining was performed on all three cell lines tested, WM115, WM239, and HUVECs, with and without exogenously added VEGF for the presence of native VEGFR2 and phosphorylated VEGFR2 (at Tyr951 and Tyr1175). Images show the presence of native and phosphorylated VEGFR2 in cytoplasm and nucleus (arrows) of WM115, WM239, and HUVEC cell lines. In addition, phosphorylation of VEGFR2 at Tyr951 is observed in both the cytoplasm and nucleus, whereas the phosphorylation of VEGFR2 at Tyr1175 is observed mostly in cytoplasm. Negative controls (no primary antibody) showed no detectable staining. Scale bar, 10 μm. (B) Expression of native VEGFR2 receptor detected in the nuclear, cytosolic, and total protein lysate fractions in WM115 and WM239 cells was evaluated using Western blot analysis. α-Tubulin (cytosolic fractions) and lamin (nuclear fractions) was used for normalization purposes. Blots show the presence of VEGFR2 protein in both nuclear and cytosolic fractions, confirming immunofluorescent results.

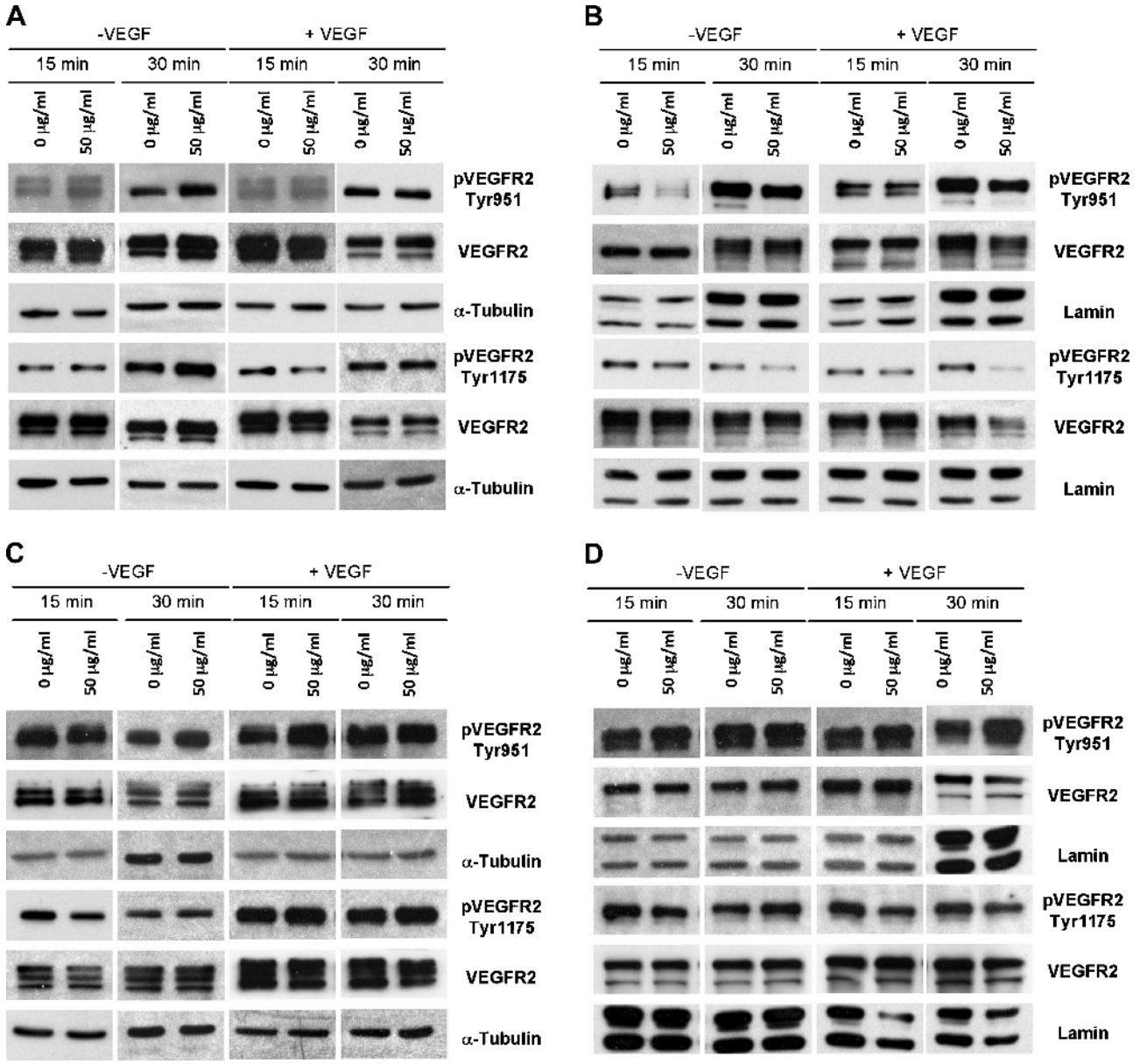

Figure 3. Effects of bevacizumab treatment on VEGFR2 phosphorylation in cytosolic and nuclear fractions of WM115 and WM239 melanoma cells *in vitro*. Addition of 50 µg/ml of bevacizumab had no significant effect on phosphorylation of VEGFR2 receptor (at Tyr951 and Tyr1175) in cytosolic fractions 15 and 30 minutes after addition (+/−VEGF) (A), whereas it significantly inhibited VEGFR2 phosphorylation at Tyr951 (both 15 and 30 minutes after addition, −VEGF) and Tyr1175 (15 minutes after addition, +VEGF) in nuclear fractions in WM115 cells (B). (C) Similarly, addition of 50 µg/ml of bevacizumab to the medium of WM239 cells only had a significant inhibitory effect on phosphorylation of VEGFR2 at Tyr1175 in cytosolic fractions after 15 minutes (−VEGF). (D) No significant change in phosphorylation of VEGFR2 (Tyr 951/1175) was observed in nuclear fractions 15 and 30 minutes after bevacizumab addition (+/−VEGF). All images shown are representative of three blots; densitometry results are shown in Table W1.

of a functional autocrine VEGF/VEGFR2 signaling loop in WM115 and WM239 cells. Immunofluorescent staining was used after an overnight starvation of WM115, WM239, and HUVECs and revealed the presence of phosphorylated (at Tyr951 and Tyr1175) and native VEGFR2 in both plasma membrane and nucleus in both WM115 and WM239 cell lines, as well as in HUVECs, used as a control endothelial cell line (Figure 2*A*). Whereas phosphorylation of VEGFR2 at Tyr951 is observed primarily in the nucleus of all three cell lines examined, phosphorylated VEGFR2 at Tyr1175 was observed mostly in the cytoplasm and the plasma membrane. Also, addition of exogenous VEGF ligand did not change the expression or the localization of native or phosphorylated VEGFR2 in any of the cell lines examined. The presence of phospho-VEGFR2 (Tyr951 and Tyr1175) in samples obtained after extensive serum starvation suggests the existence of both an autocrine and an intracrine VEGF/VEGFR2 signaling loop in both primary and metastatic melanoma cells. When total cell lysates as well as separate cytosolic and nuclear fractions were examined using Western blot analysis, VEGFR2 was observed in all samples (Figure 2*B*).

Contrary to expectations, in general, the anti–VEGF-neutralizing antibody bevacizumab failed to inhibit VEGFR2 phosphorylation in both WM115 and WM239 cells (Figure 3, *A-D*), with few exceptions.

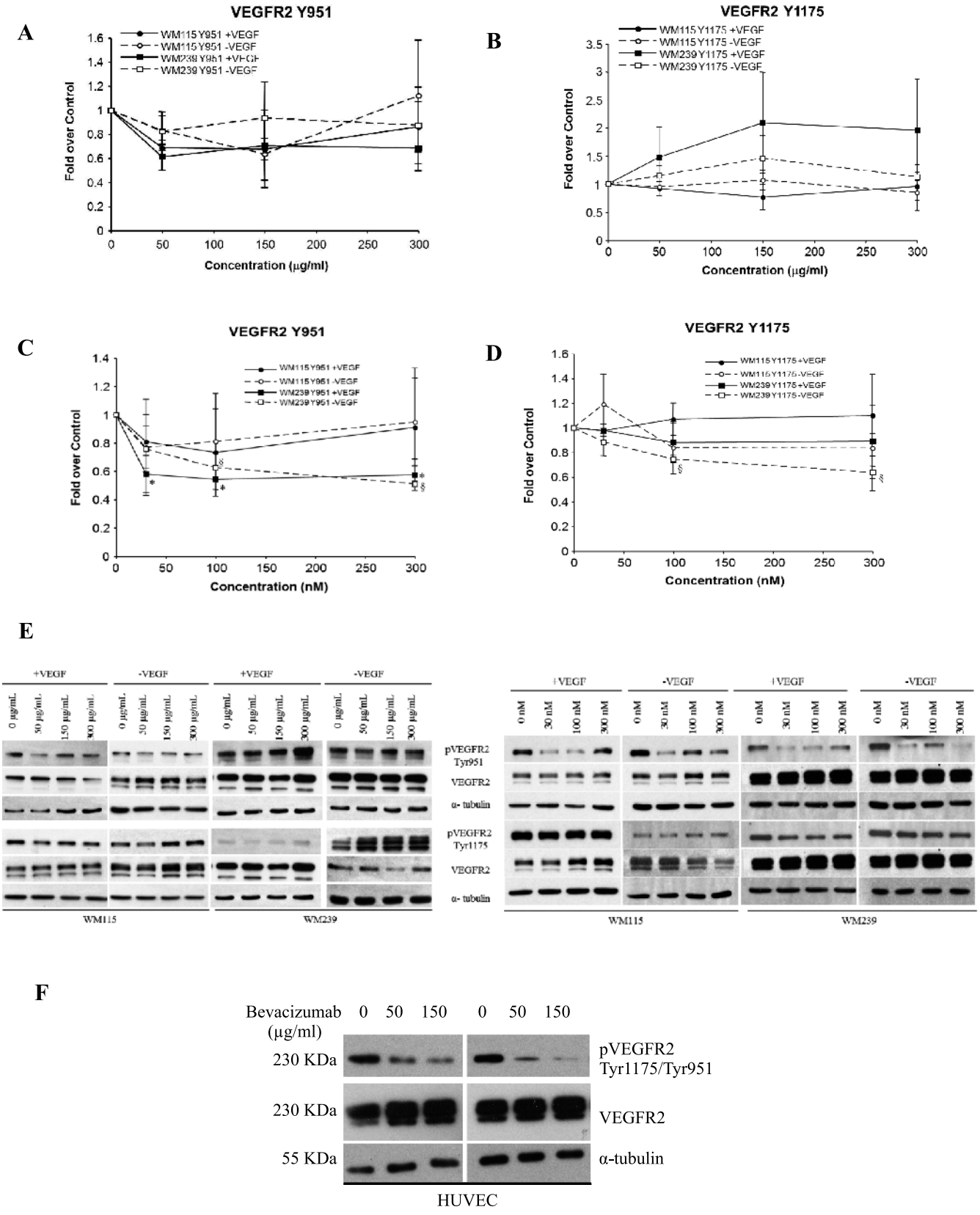

Figure 4. Dose responses to bevacizumab and sunitinib on the phosphorylation of VEGFR2 in WM115 and WM239 cells. (A, B) Neither WM115 nor WM239 cells show significant reduction in VEGFR2 phosphorylation to increasing bevacizumab concentrations (0-300 μg/ml). (C, D) Increased dosing of sunitinib (0-300 nM) had no significant effect on phosphorylation of VEGFR2 (at Tyr951/1175) in WM115 cells. On the contrary, significant inhibition of VEGFR2 phosphorylation in WM239 cells was observed at Tyr951 (+/−VEGF; *,$^{\S}P < .05$) and at Tyr1175 (−VEGF) ($^{\S}P < .05$; $n = 4$). (E) A representative Western blot of results depicted in A to D showing protein changes after bevacizumab (left) and sunitinib (right) treatment. (F) A representative Western blot shows dose-dependent (0-150 μg/ml) inhibition of VEGFR2 phosphorylation (Tyr951/1175) using bevacizumab in HUVECs. α-Tubulin was used for normalization purposes.

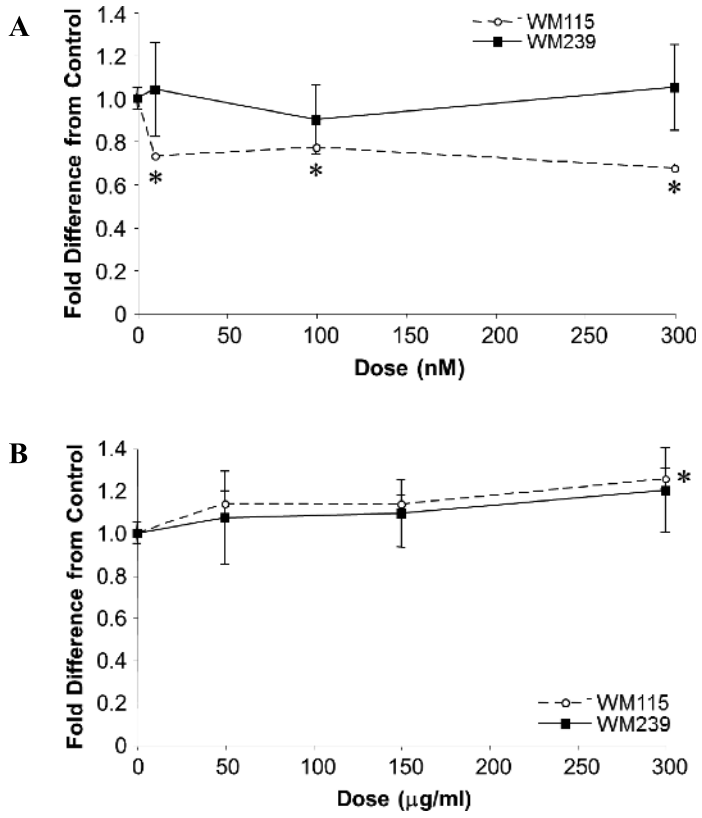

Figure 5. Effect of VEGFR2 inhibition on melanoma cell growth. (A) WM115 cells, but not WM239 cells, were susceptible to growth inhibition by sunitinib (*$P < .05$ *vs* control; $n = 3$). (B) In contrast, neither cell line was growth inhibited by bevacizumab, and WM115 cells showed significant growth enhancement at the highest dose (*$P < .05$ *vs* control; $n = 6$).

In WM115 cells, bevacizumab (at 50 μg/ml) inhibited phosphorylation of VEGFR2 at Y951, 15 and 30 minutes after addition (no exogenously VEGF added) and at Y1175 site after 15 minutes (with addition of VEGF)—as detected in nuclear fractions ($P < .05$; Figure 3*B*). Cytosolic fractions of WM115 cells treated with bevacizumab did not show inhibition of VEGFR2 phosphorylation regardless of exogenous VEGF (Figure 3*A*). In WM239 cells, bevacizumab (at 50 μg/ml) caused an inhibition of phosphorylated VEGFR2 at Y1175, 15 minutes after addition—observed only in cytosolic fractions ($P < .05$; Figure 3*C*). There was no significant inhibition of VEGFR2 phosphorylation observed in nuclear fractions (Figure 3*D*), and addition of exogenous VEGF did not affect these results.

To see if an inhibition of VEGFR2 phosphorylation is dependent on the dose of bevacizumab administered, total protein lysates were collected from WM115 and WM239 cells treated with 0, 50, 150, and 300 μg/ml of bevacizumab (Figure 4, *A*, *B*, and *E*). No significant inhibition of VEGFR2 phosphorylation was observed in either WM115 or WM239 cells (+/−VEGF) at any of the concentrations of bevacizumab. Next, cells were treated with VEGFR2 phosphorylation inhibitor sunitinib at 0, 10, 100, and 300 nM with an aim to observe dose response (Figure 4, *C-E*). Although WM115 showed no significant inhibition of phosphorylated VEGFR2 after sunitinib treatment, WM239 cells showed a significant decrease ($P < .05$) in phosphorylated VEGFR2 at Y951 (+/−VEGF) and at Y1175 (−VEGF) after sunitinib treatment.

To verify the activity of bevacizumab, we treated HUVECs with 0, 50, and 150 μg/ml bevacizumab and evaluated receptor phosphorylation. As expected, a dose-dependent reduction in phosphorylation was observed in this cell type at both Y951 and Y1175 sites on VEGFR2 (Figure 4*F*).

Sunitinib, but Not Bevacizumab, Decreases Cell Proliferation of Melanoma Cells

Along with detection of phosphorylated VEGFR2 changes, proliferation assays were performed to assess relative cell growth of melanoma cells in response to an increased doses of bevacizumab (0, 50, 150, and 300 μm/ml) as well sunitinib (0, 10, 100, and 300 nM; Figure 5). Sunitinib treatment caused significant reduction in cell proliferation compared with controls in WM239 but not in WM115 cell line ($P < .05$; Figure 5*A*). Bevacizumab treatment not only failed to inhibit cell proliferation in both cell lines but also increased their growth at the highest dosage of 300 μg/ml ($P < .05$; Figure 5*B*).

Bevacizumab Is Antiangiogenic in Primary and Metastatic Melanoma Xenografts

To test the functionality of VEGF/VEGFR2 autocrine signaling loop and evaluate the therapeutic properties of bevacizumab in melanoma,

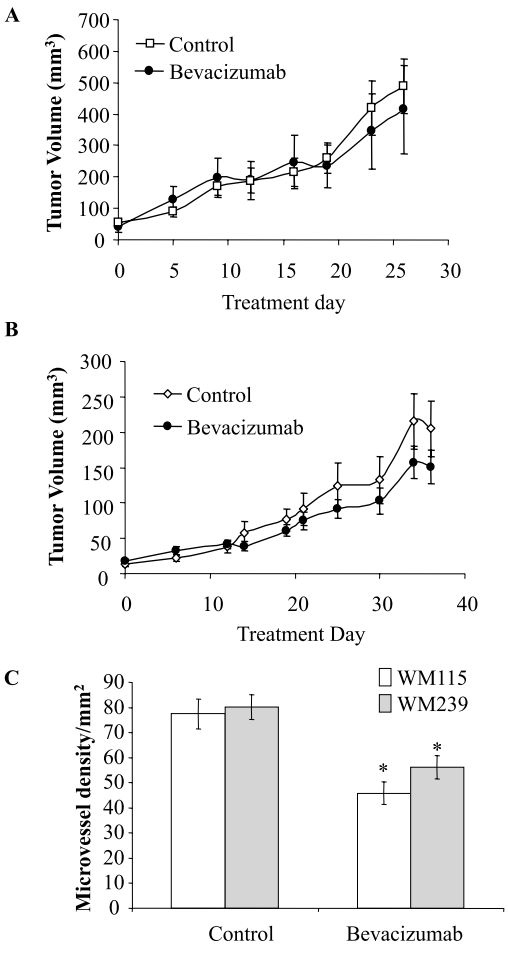

Figure 6. Impact of bevacizumab on growth of melanoma xenografts. The tumor volume in WM115 (A) and WM239 (B) xenografts did not differ significantly between control and bevacizumab-treated groups at any point during the treatment ($P \geq .05$). $n = 8$. (C) Quantification shows significant differences (*$P < .05$) in average blood vessel density between control and bevacizumab-treated groups for both cell lines.

we used this agent to treat mice bearing WM115 and WM239 melanoma xenografts. There were no significant differences in average tumor volume in bevacizumab-treated mice compared with control for either primary melanoma (WM115) or metastatic melanoma (WM239; Figure 6, *A* and *B*). For WM115, control tumors were 1.2-fold larger than treated at end point, and for WM239, control tumors were 1.4-fold larger than treated at end point; these differences were not significant ($P > .05$). However, immunofluorescence for the pan-endothelial marker CD31 revealed significant differences ($P < .05$) in blood vessel density between melanoma xenografts treated with bevacizumab *versus* control (Figure 6*C*).

VEGFR2 expression was evaluated in tumor lysates, revealing no differences. Although there was a trend toward reduced VEGFR2 levels in bevacizumab-treated tumors, this was not significant ($P \geq .05$; Figure 7, *A* and *B*). Moreover, when we investigated the levels of VEGF ligand in WM115 and WM239 xenografts treated with or without bevacizumab, we observed that bevacizumab-treated WM239 tumors had significantly less VEGF ($P < .05$; Figure 7*C*) than control xenografts. WM115 xenografts did not show this difference ($P \geq .05$; Figure 7*C*).

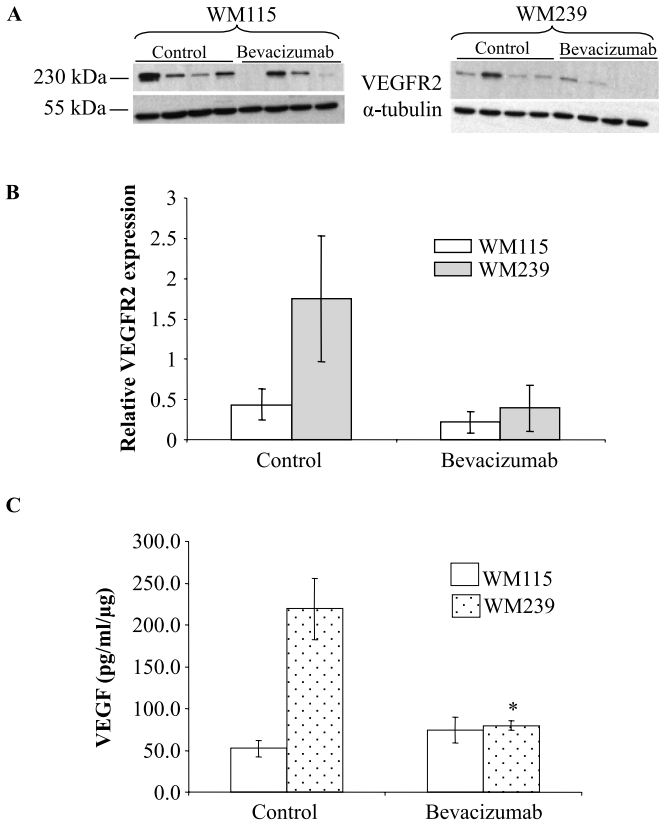

Figure 7. Expression of VEGFR2 in melanoma xenografts. (A) Representative Western blots of lysed WM115 and WM239 xenografts with quantified VEGFR2 protein expression. α-Tubulin was used for normalization purposes. (B) Densitometry shows no significant differences ($P \geq .05$) between control and bevacizumab-treated groups in expression of VEGFR2 receptor. $n = 4$. (C) When VEGF was quantified in lysed tumor xenografts using ELISA, significant differences (*$P < .05$) were observed in the levels of VEGF in bevacizumab-treated group compared with control for WM239 tumors but not WM115. $n = 3$.

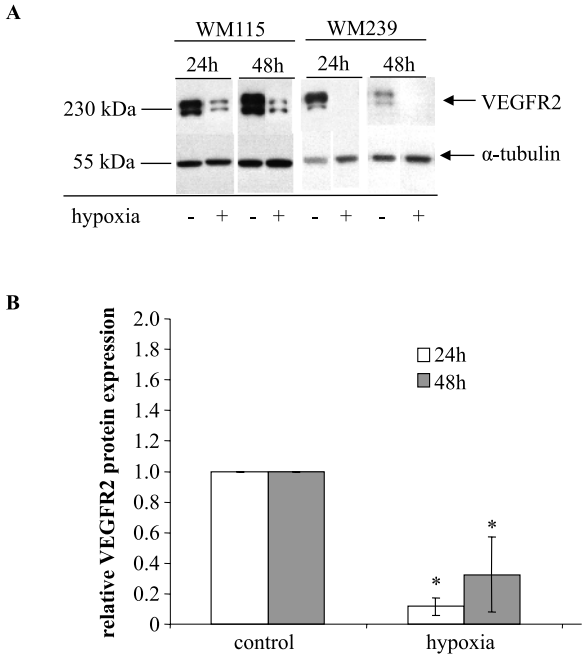

Figure 8. Expression of VEGFR2 receptor under hypoxic conditions *in vitro*. (A) Representative, composite blots showing the expression of VEGFR2 receptor in primary (WM115) and metastatic (WM239) melanoma cells when exposed in 24 and 48 hours of hypoxia. α-Tubulin was used for normalization purposes. (B) Quantification of expression demonstrates significant decrease in VEGFR2 levels in WM115 melanoma cells when exposed to hypoxia for 24 and 48 hours. *$P < .05$. $n = 3$. VEGFR2 expression was undetectable in WM239 cells exposed to hypoxia (densitometry not shown).

Down-regulation of VEGFR2 in Severe Hypoxia

Western blot analysis of melanoma cell lysates revealed that severe *in vitro* hypoxia ($O_2 < 0.01\%$) produced a significantly ($P < .05$) decreased expression of VEGFR2 receptor in WM115 and WM239 melanoma cells at both 24 and 48 hours. In fact, hypoxia almost completely diminished WM239 expression of VEGFR2 (Figure 8, *A* and *B*).

Discussion

Although endothelial signaling of VEGF ligand via VEGFR2 is well characterized in tumor vasculature, VEGFR2 signaling on cancer cells themselves is less understood, despite the fact that the expression of VEGFR2 by different types of cancer cells has been well documented in the past decade [27,35–38]. However, the concomitant expression of VEGF and VEGFR2 suggests modulation of biologic effects, such as cell survival and cell migration, in an autocrine fashion [24–26,29,37,39]. An autocrine VEGF/VEGFR2 signaling loop in breast cancer has been associated with increased activation of p38 MAPK [23]. Some melanoma cells express VEGFR2, where it may function as a mediator of the mitogenic effects of VEGF, but normal melanocytes completely lack the expression of either VEGF or VEGFR2 [21,40].

We found a functional autocrine VEGF/VEGFR2 signaling loop in human malignant melanoma cells and significantly lower VEGFR2 expression by cells derived from a metastatic lesion (WM239) compared to those from a primary lesion (WM115) or to normal endothelial cells. Aggressive melanoma tumor cells have been shown to

"masquerade" as other cell types and express genes associated with many other cellular phenotypes such as epithelial, pericyte, fibroblast, and hematopoietic cells [41,42]. Melanoma cells have also been reported capable of "vascular mimicry"—expression of endothelium-associated genes and formation of vascular networks similar to formation of embryonic vascular networks [43,44]. In fact, melanomas have been shown to relay on embryonic signaling pathways, such as expression of the embryonic morphogen, Nodal, part of the TGF-β superfamily. Nodal has been shown to interact with Notch4 pathway in aggressive melanomas [45,46].

We found that cells derived from metastatic melanoma secreted significantly more VEGF compared to cells derived from primary melanoma (observed in both *in vitro* and *in vivo* experiments). This is not surprising because the ability of melanomas to produce large amounts of VEGF is one of their hallmarks [27,38,47], and the hyperpermeability of the newly formed blood vessels caused by VEGF plays an important role in melanoma metastasis [47]. Human melanoma cells, which simultaneously produce VEGF and express VEGFRs, exhibit a higher spontaneous ability to invade the extracellular matrix (ECM) than melanoma cells not expressing either ligand or receptor [28]. This overproduction of VEGF may trigger VEGFR2 receptor down-regulation and degradation [48] therefore accounting for the reduced VEGFR2 levels seen in WM239 cells compared to WM115 cells.

In addition, our studies confirm that the anti-VEGF antibody, bevacizumab, is effective in neutralizing virtually all VEGF secreted by these melanoma cells [49]. Despite this, we found that treatment of human melanoma cells with bevacizumab not only failed in most instances to inhibit VEGFR2 phosphorylation *in vitro* but also actually produced *increased* cellular proliferation of melanoma cells. This phenomenon has not been reported in the literature; in fact, other studies show that bevacizumab inhibits VEGFR2 phosphorylation in tumor vessels of breast cancer [50], lung cancer [51], and human microvascular endothelial cells [52]. In support of this, we find that bevacizumab worked in an "orthodox" fashion on HUVECs in our hands. It is not clear why this reagent should show such differential response between endothelial cells expressing VEGFR2 and cancer cells expressing the same receptor. We speculate that bevacizumab may have bound to the melanoma VEGFR2, perhaps in complex with extensive soluble VEGF, leading to receptor clustering and autoactivation. Alternatively, it is possible that internalized complexes of VEGF and bevacizumab may continue to signal through VEGFR2 Tyr951 through complexes in early endosomes in these cells, as has recently been demonstrated in endothelial cells [53]. Further studies are required to elucidate this pathway in melanoma cells.

Autocrine VEGF/VEGFR2 signaling in the melanoma cells presents an attractive second compartment for targeted anti-VEGF therapy. However, when we treated our experimental melanoma tumors with a bevacizumab dose regimen shown to be effective in other human cancer xenografts [54], we did not get the expected antitumor response. Although bevacizumab caused a decrease in the microvessel density (MVD) in both xenograft types, and a reduction in VEGF levels in WM239 tumors, no inhibition of tumor growth was seen. Intrinsic nonresponsiveness to targeted antiangiogenic therapy has been reported in the clinic [6,55], and based on our findings here, we propose three non–mutually exclusive mechanisms: bevacizumab-induced VEGFR2 signaling in cancer cells (discussed above), intracrine pathways protected from antibody blockade, and down-regulation of target by tumor microenvironment.

Intracrine VEGF/VEGFR2 signaling that allows cancer cells to stimulate their own survival pathways without the need for exogenous secreted factors has been demonstrated for subsets of acute leukemia cells [21,26,37]. VEGF is also reported to act as an intracrine survival factor in breast cancer cells through its binding to VEGFR1 [30]. Although growth factors such as VEGF are generally seen as being operative at the cell surface, there is also evidence that VEGF can be translocated to the nucleus in some circumstances in endothelial cells [56]. VEGFR2 can also be internalized and remain in endosomal compartments for extended periods where it continues to be phosphorylated and activate p44/42 MAPK phosphorylation and cell proliferation of confluent endothelial monolayers [57]. Similar intracellular signaling presumably occurs in intracrine pathways, where ligand/receptor interactions are completely intracellular [58]. Such internal signaling systems imply that anti-VEGF neutralizing agents currently used clinically (such as bevacizumab and aflibercept) may not effectively block those pathways inside cancer cells. Because cancer cell expression of VEGFRs is more prevalent than originally thought, this could be a significant barrier to an effective anticancer therapy with angiogenesis factor–targeted reagents.

Refractoriness to VEGF signaling blockade in melanoma cells may also be modulated by the availability of the target protein because of microenvironmental factors such as hypoxia. It is known that, in locally advanced solid tumors, oxygen delivery is frequently reduced or even abolished owing to abnormalities of the tumor vasculature. Up to 50% to 60% of locally advanced solid tumors may exhibit hypoxic and/or anoxic tissue areas that are heterogeneously distributed within the tumor mass [59]. Hypoxia plays an important role in regulation of VEGF expression [60,61], and metastatic melanomas contain hypoxic areas arising in tissue distant from the blood supply [59]. We found that, *in vitro*, hypoxia significantly downregulated VEGFR2 expression to almost undetectable levels in metastatic melanoma cells. This down-regulation may be due to hypoxia-induced overexpression of VEGF in hypoxic conditions [60], leading to internalization and degradation of VEGFR2 by melanoma cells. This renders anti-VEGF therapies, such as bevacizumab, potentially refractory for the areas of tumors that are hypoxic and may be a reason for mixed success observed with bevacizumab in clinical trials of malignant melanoma to date. Receptor tyrosine kinase small-molecule inhibitors may be more effective in the treatment of hypoxic cells than monoclonal antibodies because of their ability to penetrate cells easier and thus treat tumors with functional intracellular autocrine VEGF signaling [25,30,62].

Taken together, our findings demonstrate that both primary and metastatic melanoma cells may have functional autocrine and intracrine VEGF/VEGFR2 signaling loops. We also found that bevacizumab is an effective antiangiogenic but not antitumorigenic agent in human melanoma xenografted to mice and that it may have undesirable effects on melanoma cells by increasing the phosphorylation of VEGFR2. These results suggest that, in the case of cancers with intracrine VEGF/VEGFR2 signaling loops, small-molecule inhibitors of VEGFR2 may be more effective than neutralizing antibodies at disease control.

Acknowledgments

The authors thank Kanwal Minhas for technical support and the staff of the Central Animal Facility, especially Jackie Rombeek, for care of the mice.

References

[1] Ferrara N (2002). Role of vascular endothelial growth factor in physiologic and pathologic angiogenesis: therapeutic implications. *Semin Oncol* **29**, 10–14.

[2] Ferrara N, Hillan KJ, and Novotny W (2005). Bevacizumab (Avastin), a humanized anti-VEGF monoclonal antibody for cancer therapy. *Biochem Biophys Res Commun* **333**, 328–335.

[3] Hurwitz H (2004). Integrating the anti–VEGF-A humanized monoclonal antibody bevacizumab with chemotherapy in advanced colorectal cancer. *Clin Colorectal Cancer* **4**, S62–S68.

[4] Hurwitz H, Fehrenbacher L, Novotny W, Cartwright T, Hainsworth J, Heim W, Berlin J, Baron A, Griffing S, Holmgren E, et al. (2004). Bevacizumab plus irinotecan, fluorouracil, and leucovorin for metastatic colorectal cancer. *N Engl J Med* **350**, 2335–2342.

[5] Dellapasqua S, Bagnardi V, Bertolini F, Sandri MT, Pastrello D, Cancello G, Montagna E, Balduzzi A, Mancuso P, Luini A, et al. (2008). Metronomic cyclophosphamide and capecitabine combined with bevacizumab in advanced breast cancer. *J Clin Oncol* **26**, 4899–4905.

[6] Miller K, Wang M, Gralow J, Dickler M, Cobleigh M, Perez EA, Shenkier T, Cella D, and Davidson NE (2007). Paclitaxel plus bevacizumab *versus* paclitaxel alone for metastatic breast cancer. *N Engl J Med* **357**, 2666–2676.

[7] Jurado JM, Sanchez A, Pajares B, Perez E, Alonso L, and Alba E (2008). Combined oral cyclophosphamide and bevacizumab in heavily pre-treated ovarian cancer. *Clin Transl Oncol* **10**, 583–586.

[8] Cohen MH, Gootenberg J, Keegan P, and Pazdur R (2007). FDA drug approval summary: bevacizumab (Avastin) plus carboplatin and paclitaxel as first-line treatment of advanced/metastatic recurrent nonsquamous non–small cell lung cancer. *Oncologist* **12**, 713–718.

[9] Yang JC, Haworth L, Sherry RM, Hwu P, Schwartzentruber DJ, Topalian SL, Steinberg SM, Chen HX, and Rosenberg SA (2003). A randomized trial of bevacizumab, an anti–vascular endothelial growth factor antibody, for metastatic renal cancer. *N Engl J Med* **349**, 427–434.

[10] Reardon DA, Desjardins A, Vredenburgh JJ, Gururangan S, Sampson JH, Sathornsumetee S, McLendon RE, Herndon JE II, Marcello JE, Norfleet J, et al. (2009). Metronomic chemotherapy with daily, oral etoposide plus bevacizumab for recurrent malignant glioma: a phase II study. *Br J Cancer* **101**, 1986–1994.

[11] McCarthy M (2003). Antiangiogenesis drug promising for metastatic colorectal cancer. *Lancet* **361**, 1959.

[12] Varker KA, Biber JE, Kefauver C, Jensen R, Lehman A, Young D, Wu H, Lesinski GB, Kendra K, Chen HX, et al. (2007). A randomized phase 2 trial of bevacizumab with or without daily low-dose interferon alfa-2b in metastatic malignant melanoma. *Ann Surg Oncol* **14**, 2367–2376.

[13] Hainsworth JD, Infante JR, Spigel DR, Peyton JD, Thompson DS, Lane CM, Clark BL, Rubin MS, Trent DF, and Burris HA III (2010). Bevacizumab and everolimus in the treatment of patients with metastatic melanoma: a phase 2 trial of the Sarah Cannon Oncology Research Consortium. *Cancer* **116**, 4122–4129.

[14] Grignol VP, Olencki T, Relekar K, Taylor C, Kibler A, Kefauver C, Wei L, Walker MJ, Chen HX, Kendra K, et al. (2011). A phase 2 trial of bevacizumab and high-dose interferon alpha 2B in metastatic melanoma. *J Immunother* **34**, 509–515.

[15] Mendel DB, Laird AD, Xin X, Louie SG, Christensen JG, Li G, Schreck RE, Abrams TJ, Ngai TJ, Lee LB, et al. (2003). *In vivo* anti-tumor activity of SU11248, a novel tyrosine kinase inhibitor targeting VEGF and PDGF receptors: determination of a pharmacokinetic/pharmacodynamic relationship. *Clin Cancer Res* **9**, 327–337.

[16] Patyna S, Laird AD, Mendel DB, O'Farrell AM, Liang C, Guan H, Vojkovsky T, Vasile S, Wang X, Chen J, et al. (2006). SU14813: a novel multiple receptor tyrosine kinase inhibitor with potent antiangiogenic and antitumor activity. *Mol Cancer Ther* **5**(7), 1774–1782.

[17] Socinski MA, Novello S, Brahmer JR, Rosell R, Sanchez JM, Belani CP, Govindan R, Atkins JN, Gillenwater HH, Pallares C, et al. (2008). Multicenter, phase II trial of sunitinib in previously treated, advanced non–small-cell lung cancer. *J Clin Oncol* **26**(4), 650–656.

[18] Abrams TJ, Murray LJ, Pesenti E, Holway VW, Colombo T, Lee LB, Cherrington JM, and Pryer NK (2003). Preclinical evaluation of the tyrosine kinase inhibitor SU11248 as a single agent and in combination with "standard of care" therapeutic agents for the treatment of breast cancer. *Mol Cancer Ther* **2**(10), 1011–1021.

[19] Motzer RJ, Michaelson MD, Rosenberg J, Bukowski RM, Curti BD, George DJ, Hudes GR, Redman BG, Margolin KA, and Wilding G (2007). Sunitinib efficacy against advanced renal cell carcinoma. *J Urol* **178**(5), 1883–1887.

[20] Neufeld G, Cohen T, Gengrinovitch S, and Poltorak Z (1999). Vascular endothelial growth factor (VEGF) and its receptors. *FASEB J* **13**, 9–22.

[21] Zachary I and Gliki G (2001). Signaling transduction mechanisms mediating biological actions of the vascular endothelial growth factor family. *Cardiovasc Res* **49**, 568–581.

[22] Zeng H, Sanyal S, and Mukhopadhyay D (2001). Tyrosine residues 951 and 1059 of vascular endothelial growth factor receptor-2 (KDR) are essential for vascular permeability factor/vascular endothelial growth factor–induced endothelium migration and proliferation, respectively. *J Biol Chem* **276**, 32714–32719.

[23] Aesoy R, Sanchez BC, Norum JH, Lewensohn R, Viktorsson K, and Linderholm B (2008). An autocrine VEGF/VEGFR2 and p38 signaling loop confers resistance to 4-hydroxytamoxifen in MCF-7 breast cancer cells. *Mol Cancer Res* **6**, 1630–1638.

[24] Neuchrist C, Erovic BM, Handisurya A, Steiner GE, Rockwell P, Gedlicka C, and Burian M (2001). Vascular endothelial growth factor receptor 2 (VEGFR2) expression in squamous cell carcinomas of the head and neck. *Laryngoscope* **111**, 1834–1841.

[25] Xia G, Kumar SR, Hawes D, Cai J, Hassanieh L, Groshen S, Zhu S, Masood R, Quinn DI, Broek D, et al. (2006). Expression and significance of vascular endothelial growth factor receptor 2 in bladder cancer. *J Urol* **175**, 1245–1252.

[26] Zhang H, Li Y, Li H, Bassi R, Jimenez X, Witte L, Bohlen P, Hicklin D, and Zhu Z (2004). Inhibition of both the autocrine and the paracrine growth of human leukemia with a fully human antibody directed against vascular endothelial growth factor receptor 2. *Leuk Lymphoma* **45**, 1887–1897.

[27] Graells J, Vinyals A, Figueras A, Llorens A, Moreno A, Marcoval J, Gonzalez FJ, and Fabra A (2004). Overproduction of VEGF concomitantly expressed with its receptors promotes growth and survival of melanoma cells through MAPK and PI3K signalling. *J Invest Dermatol* **123**, 1151–1161.

[28] Lacal PM, Ruffini F, Pagani E, and D'Atri S (2005). An autocrine loop directed by the vascular endothelial growth factor promotes invasiveness of human melanoma cells. *Int J Oncol* **27**, 1625–1632.

[29] Lazar-Molnar E, Hegyesi H, Toth S, and Falus A (2000). Autocrine and paracrine regulation by cytokines and growth factors in melanoma. *Cytokine* **12**, 547–554.

[30] Lee TH, Sen S, Sekine M, Hinton C, Fu Y, Avraham HK, and Avraham S (2007). Vascular endothelial growth factor mediates intracrine survival in human breast carcinoma cells through internally expressed VEGFR1/FLT1. *PLoS Med* **4**, e186.

[31] Samuel S, Fan F, Dang LH, Xia L, Gaur P, and Ellis LM (2011). Intracrine vascular endothelial growth factor signaling in survival and chemoresistance of human colorectal cancer cells. *Oncogene* **30**, 1205–1212.

[32] Rodeck U, Herlyn M, Menssen HD, Furlanetto RW, and Koprowsk H (1987). Metastatic but not primary melanoma cell lines grow *in vitro* independently of exogenous growth factors. *Int J Cancer* **40**, 687–690.

[33] Graham FL, Smiley J, Russell WC, and Nairn R (1977). Characteristics of a human cell line transformed by DNA from human adenovirus type 5. *J Gen Virol* **36**, 59–74.

[34] Coomber BL (1995). Suramin inhibits C6 glioma-induced angiogenesis *in vitro*. *J Cell Biochem* **58**, 199–207.

[35] Bellamy WT, Richter L, Frutiger Y, and Grogan TM (1999). Expression of vascular endothelial growth factor and its receptors in hematopoietic malignancies. *Cancer Res* **59**, 728–733.

[36] Decaussin M, Sartelet H, Robert C, Moro D, Claraz C, Brambilla C, and Brambilla E (1999). Expression of vascular endothelial growth factor (VEGF) and its two receptors (VEGF-R1-Flt1 and VEGF-R2-Flk1/KDR) in non–small cell lung carcinomas (NSCLCs): correlation with angiogenesis and survival. *J Pathol* **188**, 369–377.

[37] Dias S, Hattori K, Heissig B, Zhu Z, Wu Y, Witte L, Hicklin DJ, Tateno M, Bohlen P, Moore MA, et al. (2001). Inhibition of both paracrine and autocrine VEGF/VEGFR-2 signaling pathways is essential to induce long-term remission of xenotransplanted human leukemias. *Proc Natl Acad Sci USA* **98**, 10857–10862.

[38] Graeven U, Fiedler W, Karpinski S, Ergün S, Kilic N, Rodeck U, Schmiegel W, and Hossfeld DK (1999). Melanoma-associated expression of vascular endothelial growth factor and its receptors FLT-1 and KDR. *J Cancer Res Clin Oncol* **125**, 621–629.

[39] Sher I, Adham SA, Petrik J, and Coomber BL (2009). Autocrine VEGF-A/KDR loop protects epithelial ovarian carcinoma cells from anoikis. *Int J Cancer* **124**, 553–561.

[40] Gitay-Goren H, Halaban R, and Neufeld G (1993). Human melanoma cells but not normal melanocytes express vascular endothelial growth factor receptors. *Biochem Biophys Res Commun* **190**, 702–708.

[41] Bittner M, Meltzer P, Chen Y, Jiang Y, Seftor E, Hendrix M, Radmacher M, Simon R, Yakhini Z, Ben-Dor A, et al. (2000). Molecular classification of cutaneous malignant melanoma by gene expression profiling. *Nature* **406**, 536–540.

[42] Seftor EA, Meltzer PS, Schatteman GC, Gruman LM, Hess AR, Kirschmann DA, Seftor RE, and Hendrix MJ (2002). Expression of multiple molecular phenotypes by aggressive melanoma tumor cells: role in vasculogenic mimicry. *Crit Rev Oncol Hematol* **44**, 17–27.

[43] Folberg R, Hendrix MJ, and Maniotis AJ (2000). Vasculogenic mimicry and tumor angiogenesis. *Am J Pathol* **156**, 361–381.

[44] Folberg R and Maniotis AJ (2004). Vasculogenic mimicry. *APMIS* **112**, 508–525.

[45] Strizzi L, Hardy KM, Kirsammer GT, Gerami P, and Hendrix MJ (2011). Embryonic signaling in melanoma: potential for diagnosis and therapy. *Lab Invest* **91**, 819–824.

[46] Hardy KM, Kirschmann DA, Seftor EA, Margaryan NV, Postovit LM, Strizzi L, and Hendrix MJ (2010). Regulation of the embryonic morphogen Nodal by Notch4 facilitates manifestation of the aggressive melanoma phenotype. *Cancer Res* **70**, 10340–10350.

[47] Salven P, Heikkila P, and Joensuu H (1997). Enhanced expression of vascular endothelial growth factor in metastatic melanoma. *Br J Cancer* **76**, 930–934.

[48] Dougher M and Terman BI (1999). Autophosphorylation of KDR in the kinase domain is required for maximal VEGF-stimulated kinase activity and receptor internalization. *Oncogene* **18**, 1619–1627.

[49] Wang Y, Fei D, Vanderlaan M, and Song A (2004). Biological activity of bevacizumab, a humanized anti-VEGF antibody *in vitro*. *Angiogenesis* **7**, 335–345.

[50] Wedam SB, Low JA, Yang SX, Chow CK, Choyke P, Danforth D, Hewitt SM, Berman A, Steinberg SM, Liewehr DJ, et al. (2006). Antiangiogenic and antitumor effects of bevacizumab in patients with inflammatory and locally advanced breast cancer. *J Clin Oncol* **24**, 769–777.

[51] Inoue S, Hartman A, Branch CD, Bucana CD, Bekele BN, Stephens LC, Chada S, and Ramesh R (2007). mda-7 in combination with bevacizumab treatment produces a synergistic and complete inhibitory effect on lung tumor xenograft. *Mol Ther* **15**, 287–294.

[52] Costa R, Carneiro A, Rocha A, Pirraco A, Falcao M, Vasques L, and Soares R (2009). Bevacizumab and ranibizumab on microvascular endothelial cells: a comparative study. *J Cell Biochem* **108**, 1410–1417.

[53] Lanahan AA, Hermans K, Claes F, Kerley-Hamilton JS, Zhuang ZW, Giordano FJ, Carmeliet P, and Simons M (2010). VEGF receptor 2 endocytic trafficking regulates arterial morphogenesis. *Dev Cell* **18**, 713–724.

[54] Yanagisawa M, Yorozu K, Kurasawa M, Nakano K, Furugaki K, Yamashita Y, Mori K, and Fujimoto-Ouchi K (2010). Bevacizumab improves the delivery and efficacy of paclitaxel. *Anticancer Drugs* **21**, 687–694.

[55] Takano S, Mashiko R, Osuka S, Ishikawa E, Ohneda O, and Matsumura A (2010). Detection of failure of bevacizumab treatment for malignant glioma based on urinary matrix metalloproteinase activity. *Brain Tumor Pathol* **27**, 89–94.

[56] Li W and Keller G (2000). VEGF nuclear accumulation correlates with phenotypical changes in endothelial cells. *J Cell Sci* **113**, 1525–1534.

[57] Lampugnani MG, Orsenigo F, Gagliani MC, Tacchetti C, and Dejana E (2006). Vascular endothelial cadherin controls VEGFR-2 internalization and signaling from intracellular compartments. *J Cell Biol* **174**, 593–604.

[58] Re RN and Cook JL (2006). An intracrine view of angiogenesis. *Bioessays* **28**, 943–953.

[59] Vaupel P, Kallinowski F, and Okunieff P (1989). Blood flow, oxygen and nutrient supply, and metabolic microenvironment of human tumors: a review. *Cancer Res* **49**, 6449–6465.

[60] Detmar M, Brown LF, Berse B, Jackman RW, Elicker BM, Dvorak HF, and Claffey KP (1997). Hypoxia regulates the expression of vascular permeability factor/vascular endothelial growth factor (VPF/VEGF) and its receptors in human skin. *J Invest Dermatol* **108**, 263–268.

[61] Hicklin DJ and Ellis LM (2005). Role of the vascular endothelial growth factor pathway in tumor growth and angiogenesis. *J Clin Oncol* **23**, 1011–1027.

[62] Gerber HP, Malik AK, Solar GP, Sherman D, Liang XH, Meng G, Hong K, Marsters JC, and Ferrara N (2002). VEGF regulates haematopoietic stem cell survival by an internal autocrine loop mechanism. *Nature* **417**, 954–958.

Table W1. Quantification of Relative VEGFR2 Receptor Expression in Cytosolic and Nuclear Fractions in WM115 and WM239 Melanoma Cells Treated with Bevacizumab (50 μg/ml).

	Time (min)	pVEGFR2 Site	Exogenous VEGF	Relative Expression ± SEM
A				
Cytosolic fractions	15	Y951	–	0.98 ± 0.24
	30	Y951	–	0.86 ± 0.11
	15	Y951	+	0.92 ± 0.08
	30	Y951	+	0.94 ± 0.16
	15	Y1175	–	1.13 ± 0.24
	30	Y1175	–	0.87 ± 0.28
	15	Y1175	+	1.09 ± 0.18
	30	Y1175	+	0.88 ± 0.10
Nuclear fractions	15	Y951	–	0.81 ± 0.07*
	30	Y951	–	0.81 ± 0.02*
	15	Y951	+	0.92 ± 0.22
	30	Y951	+	1.04 ± 0.06
	15	Y1175	–	1.00 ± 0.22
	30	Y1175	–	0.83 ± 0.11
	15	Y1175	+	0.80 ± 0.02*
	30	Y1175	+	1.13 ± 0.047
B				
Cytosolic fractions	15	Y951	–	0.96 ± 0.08
	30	Y951	–	0.88 ± 0.16
	15	Y951	+	1.22 ± 0.18
	30	Y951	+	1.49 ± 0.60
	15	Y1175	–	0.83 ± 0.04*
	30	Y1175	–	1.00 ± 0.28
	15	Y1175	+	1.14 ± 0.15
	30	Y1175	+	1.29 ± 0.17
Nuclear fractions	15	Y951	–	0.97 ± 0.13
	30	Y951	–	1.00 ± 0.07
	15	Y951	+	1.05 ± 0.13
	30	Y951	+	1.27 ± 0.17
	15	Y1175	–	0.96 ± 0.08
	30	Y1175	–	0.89 ± 0.11
	15	Y1175	+	1.14 ± 0.11
	30	Y1175	+	1.15 ± 0.13

The relative expression of native and phosphorylated VEGFR2 receptor (at Y951 and Y1175 sites) was assessed at 15- and 30-minute time points after bevacizumab addition, with or without exogenous VEGF. (A) Addition of bevacizumab had no significant ($P > .05$) effect on the phosphorylation of VEGFR2 receptor (Y951/Y1175) in cytosolic fractions 15 and 30 minutes after addition (±VEGF), whereas it significantly (*$P < .05$) inhibited VEGFR2 phosphorylation at Y951 (both 15 and 30 minutes after addition, –VEGF) and Y1175 (15 minutes after addition, +VEGF) in nuclear fractions in WM115 cells (*$P < .05$). (B) Similarly, addition of bevacizumab to the medium of WM239 cells only had a significant inhibitory effect on the phosphorylation of VEGFR2 at Y1175 in cytosolic fractions after 15 minutes (–VEGF; *$P < .05$). No significant change in phosphorylation of VEGFR2 (Y951/Y1175) was observed in nuclear fractions 15 and 30 minutes after bevacizumab addition (±VEGF; $P > .05$).